Jordan Journal of Pharmaceutical Sciences, Volume 15, No. 2, 2022

Molecular modeling studies of some phytoligands from *Ficus sycomorus* fraction as potential inhibitors of cytochrome *CYP6P3* enzyme of *Anopheles coluzzii*

Abba Babandi[1,2*], Chioma A. Anosike[2], Lawrence U.S. Ezeanyika[2], Kemal Yelekçi[3], Abdullahi Ibrahim Uba[4*]

[1]Department of Biochemistry, Bayero University, Nigeria
[2]Department of Biochemistry, University of Nigeria, Nsukka**,** Nigeria
[3]Department of Bioinformatics and Genetics, Faculty of Engineering and Natural Science, Kadir Has University, Turkey
[4]Complex Systems Division, Beijing Computational Science Research Center, China

ABSTRACT

The major obstacle in controlling malaria is the mosquito's resistance to insecticides, including pyrethroids. The resistance is mainly due to the over-expression of detoxification enzymes such as cytochromes. Insecticides tolerance can be reduced by inhibitors of P450s involved in insecticide detoxification. Here, to design potential CYP6P3 inhibitors, a homology model of the enzyme was constructed using the crystal structure of retinoic acid-bound cyanobacterial CYP120A1 (PDB ID: 2VE3; Resolution: 2.1 Å). Molecular docking study and computational modeling were employed to determine the inhibitory potentials of some phytoligands isolated from *Ficus sycomorus* against *Anopheles coluzzii* modeled P450 isoforms, *CYP6P3*, implicated in resistance. Potential ligand optimization (LE) properties were analyzed using standard mathematical models. Compounds 5, 8,and 9 bound to the Heme iron of *CYP6P3* within 3.14, 2.47 and 2.59 Å, respectively. Their respective binding energies were estimated to be -8.93, -10.44, and -12.56 Kcal/mol. To examine the stability of their binding mode, the resulting docking complexes of these compounds with *CYP6P3* were subjected to 50 ns MD simulation. The compounds remained bound to the enzyme and Fe (Heme):O (Ligand) distance appeared to be maintained over time. The coordination of a strong ligand to the heme iron shifts the iron from the high- to the stable low-spin form and prevented oxygen from binding to the heme thereby inhibiting the catalytic activity. The LE index showed the high potential of these compounds (5 and 8) to provide a core fragment for optimization into potent P450 inhibitors.

Keywords: Homology modeling; CYP6P3; Molecular docking; Molecular dynamics simulation ligand efficiency; CYP6P3 inhibitors.

INTRODUCTION

Malaria vector control strategy generally uses traditional approach to decrease global malaria cases. These measures include space spraying, indoor residual spraying, long-lasting insecticidal nets, larval source management, bio-larvicide application, etc [(1)]. The world health organization (WHO) recommends the use of pyrethroid insecticides only for adult mosquitoes in current vector control program [(1)(2)]. In recent times, resistance of the adult mosquitoes to these insecticides was reported widely, making research targeted at new classes of insecticides incredibly important [(1)(3)]. Also, some insecticides/pesticides have apparent environmental shortcomings, due to their persistence in the surroundings. These persistent insecticides are prone to resistance by

[*]***Corresponding author:***
Abba Babandi, Abdullahi Ibrahim Uba
ababandi.bch@buk.edu.ng , aiuba@csrc.ac.cn
Received on 25/8/2021 and Accepted for Publication on 26/12/2021.

insects much more commonly than non-persistent insecticides. Photo-degradation by sunlight is one of the pathways that destroy pesticides when release to the environment [4].

Cytochrome (P450) monooxygenase, a protein of 45–55-kDa, is a structurally different family of hydrophobic, heme-containing, membrane associated enzymes involved in the metabolism of xenobiotics such as insecticides in mosquitoes, thereby causing resistance. In insects, P450s are inducible and metabolize diverse collection of substrates. This usually results in the detoxification of the insecticide to more soluble and less toxic forms. Thus, P450s play important role in numerous aspects of insect biology, physiology and the insecticide resistance [5][6]. The resistance linked to P450s occurs probably due to gene(s) over expression [6]. Cis- and trans-regulating factors involved in P450 gene expression are also implicated in the insecticide resistance. This may be responsible for the resistance and consequences of malaria cases in the region. The mosquitoes have a genomic collection of over 100 P450 genes [7][8][9], that can mount defense against the insecticides leading to insecticide resistance. The *CYP6* family of P450 enzymes has been reported to be up-regulated in the majority insecticide resistant malarial vectors [10]. *CYP6M2*, *CYP325A3*, **CYP6Z1**, **CYP6Z2** *CYP6Z3*, *CYP6P3*, **CYP9K1** and *CYP4G16* [10][11][12][13], has been established to be up-regulated in adults pyrethyroids resistant mosquito strains. These enzymes are recognized for mono-oxygenase activities, in which they catalyze the transfer of one atom of molecular oxygen (O_2) to a substrate (e.g., insecticides) and reducing the other oxygen to water during the reaction. They also show other catalytic properties such as being oxidases, reductases, desaturases, dealkyalases, isomerases, C-C cleavage and dimerization reactions [14].

P450s almost always act as monooxygenases, or mixed-function oxidases, using the stoichiometric mechanism shown in equation (1).The reaction utilizes the pyridine nucleotide NADH or NADPH as a cofactor which deliver electrons via a flavoprotein or an iron-sulfur protein. [15]

$$\mathbf{R + NAD(P)H + O_2 \longrightarrow NAD(P)^+ + RO + H_2O} \quad \ldots\ldots(1)$$

Where: R is the insecticide or xenobiotics.

The P450s enzymes are generally inhibited by mechanism-based inhibition through covalent modifications of the active site amino acid residues and / or the central heme group of the enzyme which result to irreversible enzyme inhibition [16]. This P450s inhibition leads to prevention of insecticides detoxification in mosquitoes and restore the efficacy of the insecticides in mosquitoes' resistance strains. The most frequently use P450s inhibitor nowadays is Piperonyl butoxide (PBO). It has being use as insecticide synergist of pyrethroids against mosquito vectors [17][18]. Additive or synergistic applications through combination of PBO and another insecticide such as pyrethroids with different mode of action may completely restore the efficacy of pyrethroid insecticides on resistant *Anopheles* mosquitoes [19][20].The PBO have reported to have some environmental, non-target organisms and human toxicities [21][22]. As such, it warrants formulating a new insecticides or synergists or potentiating agents that are human and eco-friendly [20].

Over-expression of *CYP6P3* isoform of P450 has been reported in Benin and Nigeria malaria vectors [23]. The *CYP6P3* isoform is known to metabolize insecticide such as pyrethroids and bandiocarb [24][25]. After many decades of insecticides pressure, mosquito populations have become resistant to multiple chemical insecticide families, compromising the effectiveness of chemical-based control [26]. Many insecticides, including the organochlorines, organophosphates and carbamates, persist in the environment as toxic waste [27] and are neurotoxic not only to humans, but to livestock [28]. Furthermore, the redundant mode of action of insecticides may accelerate the emergence of cross-resistance to other insecticides [27].

The resistance of insects to insecticides can be minimized or enhanced by inhibitors of cytochrome P450s

involved in insecticide detoxification. Today, there is an urgency to develop alternative control methods, including novel insecticides, to better manage resistance and maintain effective tools for fighting vector-borne diseases such as malaria. Insights into molecular mechanisms of interactions of natural compounds with some mosquito P450s implicated in resistance can be of important for the rational design of new insecticides or insecticide synergists, and for insecticide resistance management control of malaria vectors. The insecticidal and acricidal activities of plant called *Ficus sycomorus* have been reported by Rhome [(29)]. The study identified 22 main compounds in the leaf extract that were more toxic in fumigant toxicity test than contact phase to insects. *Ficus benghalensis* and *Ficus sarmentosa var. henryi* were proven to have larvicidal activities against different larval stages of both *Culex* and *Anopheles* mosquitoes [(30)].

Phytochemicals act at multiple, novel target sites [(31)(32)(33)(34)], thereby reducing the potential for resistance [(32)(35)(36)]. Some bioactive compounds, rhinacanthin-A, -B, and –C (Figure 1), isolated from *Rhinacanthus nasutus* exhibited potent inhibitory activity against both CYP6AA3 and CYP6P7 isoform from *Spodoptera frugiperda* cells [(37)].

Natural insecticides such as azadirachtin, pyrethrins, rotenone, spinosad and abamectin were proved to be effective against insects [(38)]. But selectivity durability and safety of botanical insecticides are not total and some natural insecticidal compounds are very toxic to humans and non target organisms [(38)]. Pyrethrum or pyrethrins, extracted from *Chrysanthemum cineraria* seed has been used locally as an insecticide to control insects for centuries. The pyrethrins are particularly labile when exposed to the UV element of sunlight (Fig. 1). This fact significantly restricted the use of this natural insecticide outdoors. A study previously reported the pyrethrins half-life on tomato and bell pepper fruits grown in a field were 2 h or less than that [(39)]. This problem of pyrethrins labiality created the need for the search of new or development of synthetic derivatives that are more stable in sunlight, effective, non-toxic to non-target organisms and eco-friendly.

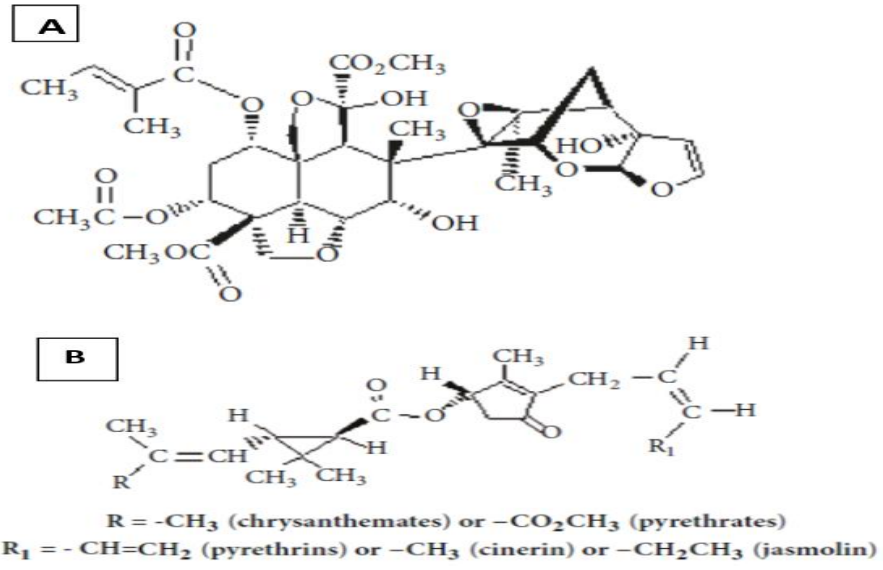

Figure 1. Chemical structures of some natural insecticides: Azadirachtin (B) and Pyrethrins and its derivatives (B) [(38)].

According to Jones et al.[40], understanding the complexity of insecticide resistance mediated by P450s relies on homology modeling since the crystal structures is not available. Such modeling, as explained by de Graaf *et al*. [41], has greatly improved the understanding of the complexity of insecticide resistance. In this study, homology model of *CYP6P3* is built and binding of *Ficus sycomorus* phytoligands to the protein was investigated using molecular docking. Molecular docking allows for prediction of binding mode and binding affinity of these potential inhibitors. Ligand efficiency (LE) calculation was performed to further evaluate the potency of the compounds. Molecular dynamics simulation was used to rapidly validate results obtained from both docking and LE calculation.

Methods

Computational Methods

Homology modeling and system setting

FASTA sequence files of the target proteins were retrieved from the Uniprot database [42]. Crystal structure of retinoic acid bound cyanobacterial CYP120 A1 (PDB ID: 2VE3; Resolution: 2.1 Å) was retrieved from the protein data bank [43]. Modeler structure prediction software [44] was used to construct the homology model of mosquito's *CYP6P3*. Structural validation was carried out using ProSAweb server (https://prosa. services. came. sbg. ac.at/prosa.php) on which the overall quality of the model was calculated by comparing its z-score with the z-score values of the protein structures determined experimentally. This model was found to be within the region of structures determined by X-ray crystallography (Figure 2A), and with minimum residual energy content (Figure 2B). The model was then prepared, preprocessed, corrected the bond orders, added hydrogens and disulfide bonds where necessary, assign correct atom charges based on the protonation state using predicted pKa values at physiological pH. The charge state was optimized, and restrained minimization was carried out.

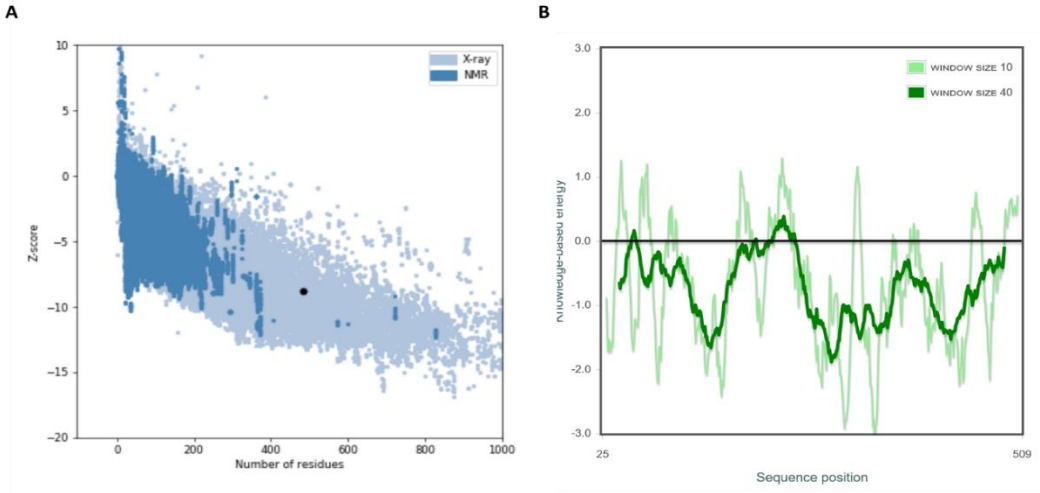

Figure 2. Structural validation of the best model: ProSA-web z-scores of protein chains from protein data bank that were determined by X-ray crystallography (light blue) and NMR spectroscopy (dark blue) with respect to their length. The plot showed that CYP6P3 (black spot) with the z-score value -8.00 is within the range of native conformation (A). The energy plot showing the local model quality by plotting energies as a function of amino acid sequence position i—positive values correspond to erroneous parts of the model (B).

Molecular docking and ligand optimization calculation

Dockings were done using the Glide software [45]. The extra precision (XP) scoring function of the GLIDE was used to model ligand-protein interaction with increased accuracy [46][47]. The template crystal structures were used to create docking grid file. The grid file was generated using a van der Waals scaling factor of 1 and a partial charge cutoff of 0.25. Ligands were docked into the generated grid of the protein receptor using an OPLS3 force field and their docking scores were calculated using Glide XP scoring function [48].

The XPG score optimized the ligand binding energy on the behalf of the force field parameters, and penalties that had significant influences over the receptor-ligand binding. The following equation denotes the formulae for XPG calculations.

Score= a*vdW+b*Coul+Lipo+Hbond+Metal+BuryP+RotB+Site…….(2)

Where: vdW, Coul, Lipo, H bond, metal, BuryP, Rot B, and Site denote van der Waals energy, Coulomb energy, lipophilic contacts, hydrogen-bonding, metal-binding, penalty for buried polar groups, penalty for freezing the rotatable bonds, and polar interactions with the residues in the active site, respectively; a = 0.065 and b = 0.130 are coefficient constants of van der Waals energy and Coulomb energy, respectively.

Ligand optimization predictions

The Ligands optimization parameters were determined using mathematical equations below:

$Ki = 10(\Delta G/1.366)$ [49]…… .(3)

$LE = \Delta G° / HA = (-2.303RT/HA) \times \log(Kd/C°)$ (LE ≥0.3)[50]…… ……..(4)

Where: $\Delta Go = -2.303RT \times \log (Kd/C°)$

R is the ideal gas constant ($1.987x10^{-3}$ kcal/K/mol) and **T** is the temperature in Kelvin (K), Co is the standard concentration, and Kd is the binding constant.

The above formulae assumed that the binding ΔG is directly proportional to the number of heavy atoms or non-hydrogen atoms in the ligand. And the standard reference assumption for the formulae is aqueous solution at 300 K, pH = 7, all other concentrations being 1 M. At this experimental state, the formulae term -2.303RT is approximately -1.37 kcal/mol, when the Kd is expressed as the logarithm to base 10 (log Kd). LE does not state that a change in the heavy atom count of +1 results in a log order change in affinity (pKd=1) [51]. Projected suitable values of LE for good candidates are >~0.3 kcal/mol/non-hydrogen atom (HA) (based on a <10nM molecule having HA of 38 (~500 Da) [52] and cLogP (Desolvation) of <3 [53].

To play down the important of ligand size in the binding affinity, two size-independent modifications of LE indices using heavy atom count only have been proposed. These are Fit Quality (FQ) [54] and Size Independent Ligand Efficiency (SILE) [55].

Fit Quality (FQ) = LE/LE_{scale}……(5)

$LE_{scale} = 0.873e^{-0.026 \times HA} - (0.064)$ (FQ ≥0.8 as hit) [52]……..(6)

SILE = pIC50 or pKi ÷ $HA^{0.3}$ ……(7)

Or = $-RT\ln (pKi)/ (NHA)^{0.3}$……(8)

Reducing the ligand size and lipophilicity tends to increase ligand efficiencies, and the individual target datum suggests that doing so may not necessarily be detrimental to affinity for many targets.

Molecular dynamics simulation

The free form of *CYP6P3* enzyme and its docking complexes with compounds 5, 8, and 9 were prepared for MD simulation. Input files were generated using CHARMM-GUI server (http://www.charmm.org) [56], via which the ligands were parameterized using CHARMM General Force Field (CGenFF) server (https://cgenff.paramchem.org/) [57]. MD simulation was performed using Nanoscale MD (NAMD) software [58]. A 1000-steps minimization by steepest descent method; 5 ns equilibration in standard number of particles, volume, and temperature (NVT) ensemble; and unrestrained 50 ns-

production MD simulations in standard number of particles, pressure, and temperature (NPT) ensemble were performed. The simulation was carried out at 2 fs time scale, and the trajectory frame was collected every 100 ps. To identify the dominant structure, each trajectory was clustered using RMSD cutoff of 3.0 Å using Chimera[59]. Ligand binding mode stability was assessed by computing root mean-square deviation (RMSD), root mean-square fluctuation (RMSF), radius of gyration (Rg), and Fe (Heme)- O(Ligand) distance over the entire simulation period.

Results

Molecular docking of phytoligands in the active site of *CYP6P3* is presented in table 1 below. Eight (8) compounds from the GC-MS analysis of active fraction of *F. sycomorus* with 1 standard inhibitor (Compound 9- the PB0) (Fig. 3) were docked into the active site of the enzyme. The binding energies for compound 1, 2, 5, 8 and 9 were 3.77, 2.89, 8.93, 10.44 and 12.56 Kcal/mol, respectively. However, compounds 3, 4, 6 and 7 were too large to fit into the active site of the *CYP6P3*. Compounds 5, 8 and 9 bound to the heme-iron at a regioselective distance or putative hydroxylation sites of 3.14 Å (Fig. 4), 2.47 Å (Fig. 5) and 2.59 Å (Fig. 6), respectively, which is less than the maximum distance required for reactivity (6 Å) with Fe-atom of the heme group. The common interacting amino acid residues in the binding pocket were *Phe123*, *Val310*, *Pro379* and *Val380* (Fig. 4-6). These and other residues contributed to the stability of the enzyme-ligand interactions via hydrophobic and π-π interactions (Fig. 4-6). Estimating the binding affinity of a small molecule in the active site of the receptor helps to understand ligand-protein interaction. These molecular interactions occur through hydrogen bond and phi-interaction. Phyto-ligands 5and 8 bound well to the heme iron at close distance to *CYP6P3* and thus may be potential inhibitors (Table 1). The amino acid residues such as *Phe123* close to the heme/porphyrin of the modeled *CYP6P3* indicates that it may be involve in π-π interactions with the heme ring, and make available, the electrons that can be supplied for the formation of the activated and stabilizing oxygen atom during the reaction with the ligand (Fig. 4-6). Other amino acid residues lining the active site have no π-electron to contribute except for the hydrophobic side chains (Fig. 4-6). These side chains could be engaged in steric interaction with the heme group (Fig. 4-6).

Table 1: Binding energies and Ligand-heme iron Distance of *CYP6P3* interactions with *F. sycomorus* phytoligands

Compounds	Name of Ligand	ΔG (Kcal/mol)	Distance from heme (Å)
1	Dodecane, 4,6-dimethyl-	-3.77	-
2	Heptadecane	-2.89	-
3	Eicosane	Non-inhibitor	-
4	4,8,12,16-Tetramethylheptadecan-4-olide	Non-inhibitor	-
5	Bis(2-ethylhexyl) phthalate	-8.93	3.14
6	Tetracontane	Non-inhibitor	-
7	Squalene	Non-inhibitor	-
8	Sigmasterol	-10.44	2.47
9	Piperonyl butoxide (PBO)	-12.56	2.59

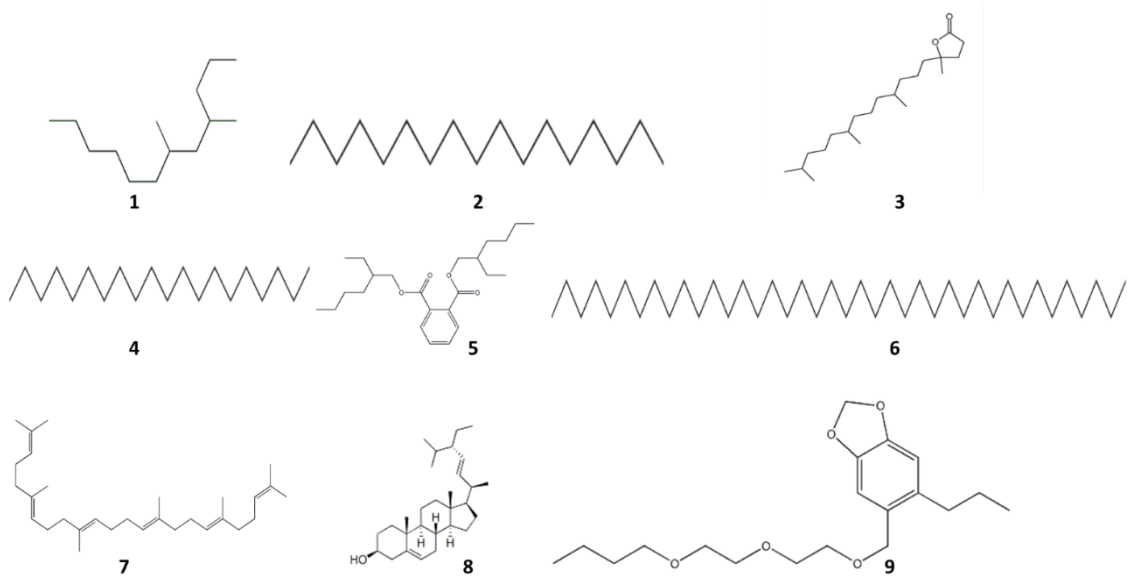

Figure 3. The phytoligands from active fraction of *Ficus sycomorus* obtained from GC-MS analysis.

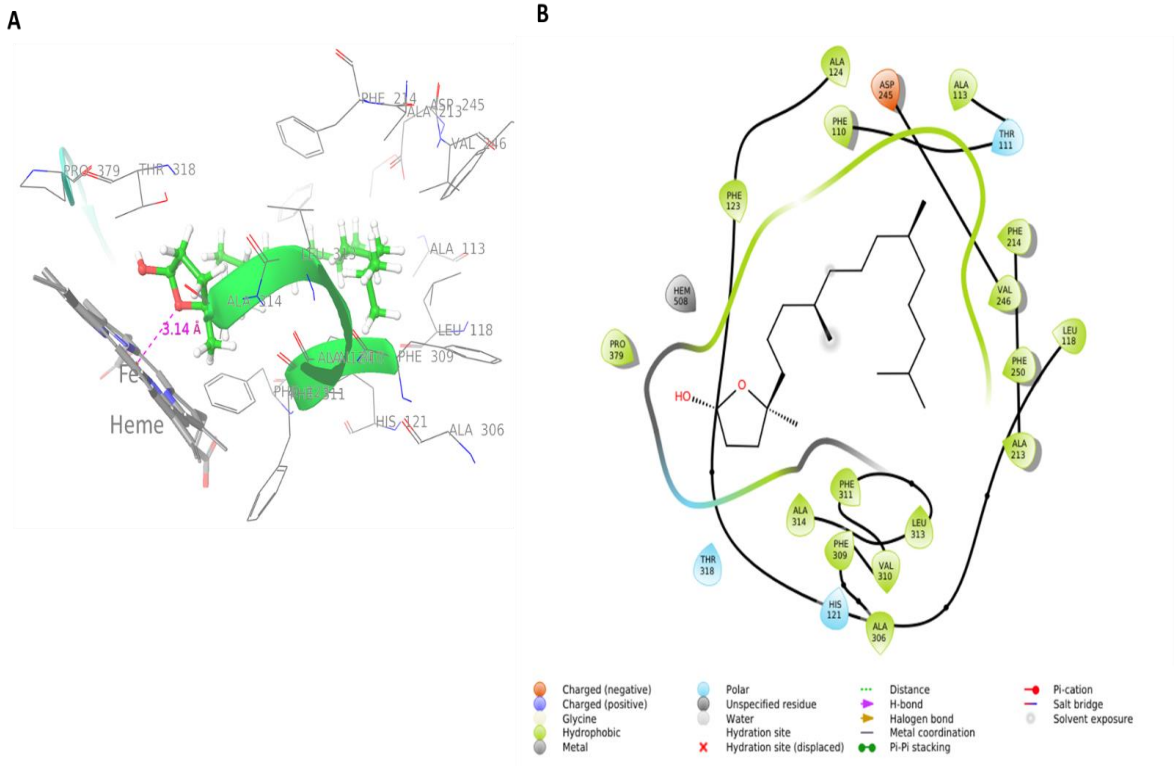

Figure 4. Docking pose and interaction diagram of compounds 5 with *CYP6P3*. Compound 5 bound to *CYP6P3* by coordinating with Fe^{2+} of the heme group via oxygen and hydroxyl groups.

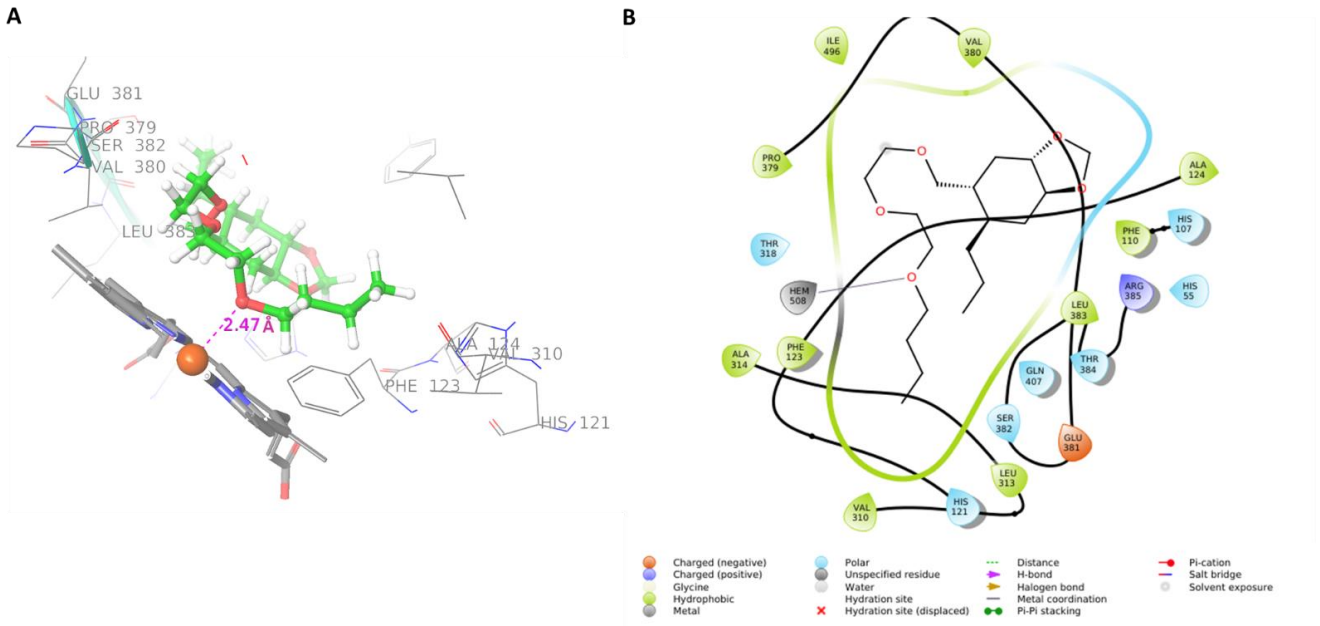

Figure 5. Docking pose and interaction diagram of compounds 8. Compound 8 bound to *CYP6P3* by coordinating with Fe^{2+} of the heme group via oxygen and hydroxyl groups.

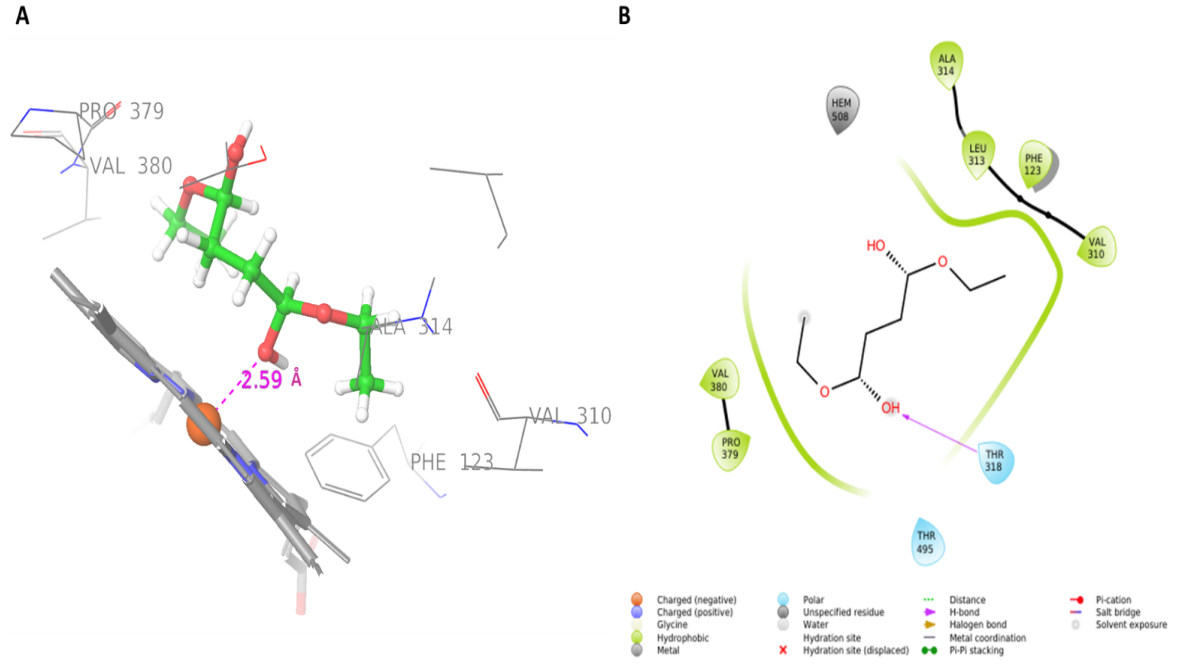

Figure 6. Docking pose and interaction diagram of compounds 9. Compound 9 bound to *CYP6P3* by coordinating with Fe^{2+} of the heme group via oxygen and hydroxyl groups.

Ligand optimization prediction

From molecular docking studies, most of the pytoligands appeared to be too big to fit into the active site of the enzymes generally due to molecular structure and size. The ligand optimization potentials of these promising fragments were evaluated, and the result is presented in Table 2. The ligand efficiency parameters: ligand efficiency, size independent ligand efficiency and Fit quality potentials of the fragments from *F. sycomorus* active fraction (LE, SILE and FQ) showed characteristics potential for molecular optimization.

Table 2: Physiochemical/bioactivity prediction of Phytoligands from *F. sycomorus* for potential optimization

Compound	Ki(M)	LE(kJ/mol/HA	SILE	LEscale	FQ
1	27.60	0.27	12.49	0.54	3.65
2	21.16	0.17	9.04	0.50	2.48
5	65.37	0.37	24.03	0.36	6.47
8	76.43	0.36	27.59	0.34	7.50
9	-	-	-	-	-

Compounds 5 and 8 have LE of 0.37 and HA of 0.36 kcal/mol/, respectively. This is within the range of standard LE of developable drug fragment (≥ 0.3Kcal/mol/HA). While compound 1 can be enhanced, compound 2 appears to be poor target fragment with LE 0.17 kcal/mol/HA (Table 2). The SILE and FQ of these phytoligands were good with the best being compound 8 (FQ= 7.50; SILE = 27.59) and can be good starting material for optimizations.

Molecular dynamics simulation

Molecular dynamics simulation has proven to be a powerful tool used for examining the stability of ligand binding mode [(60)] The four systems simulated showed increased RMSD trend until halfway through the simulation, beyond which convergence was reached until the end of the simulation (Fig. 7A). This increased RMSD trend of the modeled structure of *CYP6P3* showed structural adjustment and transition to potential active structure [(61)]. Nevertheless, the ligands slightly reduced the structural deviation toward the end of the simulation. These trends are consistent with residual fluctuation (RMSF) (Fig. 7B), and radius of gyration—a measure of protein structural compactness (Fig. 7C). Furthermore, owing to the potential role of Fe^{2+}coordination by ligand, timeline of distance between Fe^{2+} and O on the ligands was computed. This distance showed stable trends (especially, for compound 8 and 9) over time (Fig. 7D).

Trajectory clustering identified dominant structure representing 78%, 69% and 64% respectively, compound 5, 8, and 9 systems. For these structures, the Fe^{2+}:O distance was found to be 2.98 (Fig. 8A), 2.77 (Fig. 8B) and 2.27 Å (Fig. 8C) respectively, for compound 5, 8, and 9.

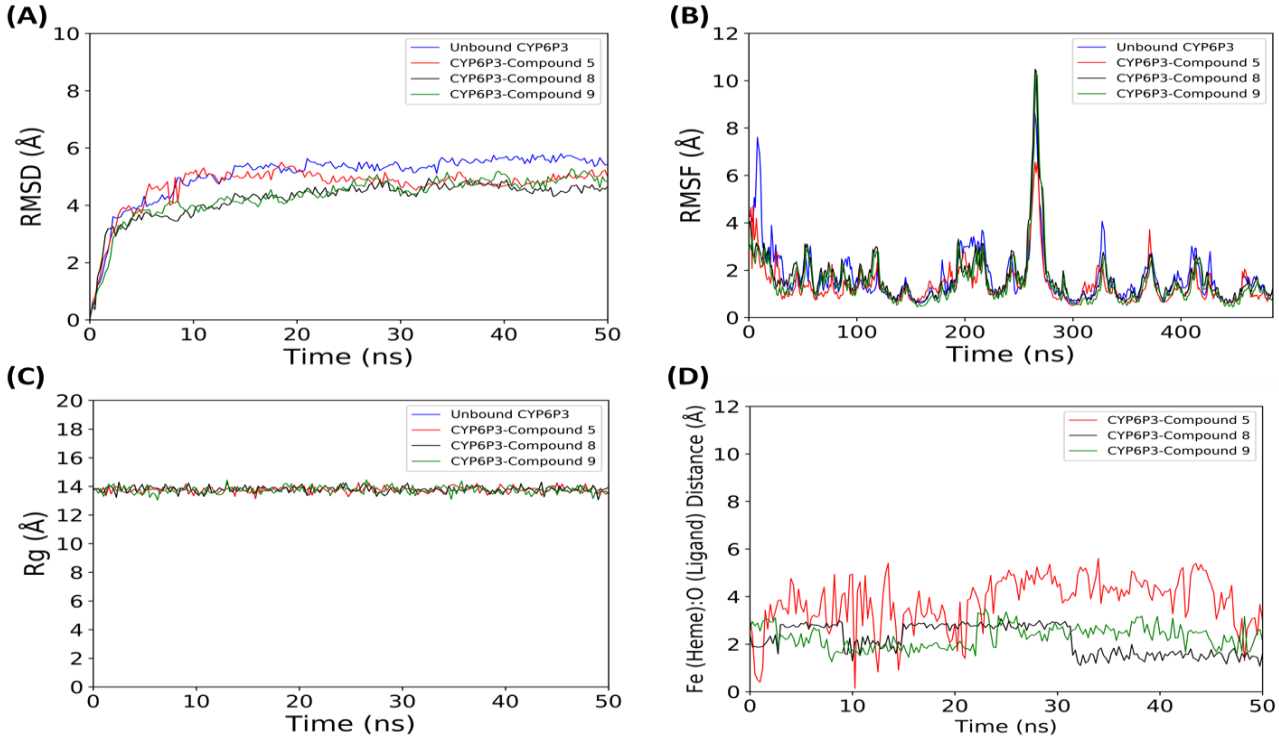

Figure 7. Molecular dynamics simulation results: (A) root mean-square deviation (RMSD) (B); root mean-square fluctuation (RMSF); (C) radius of gyration; and (D) Fe^{2+}:O distance profiles.

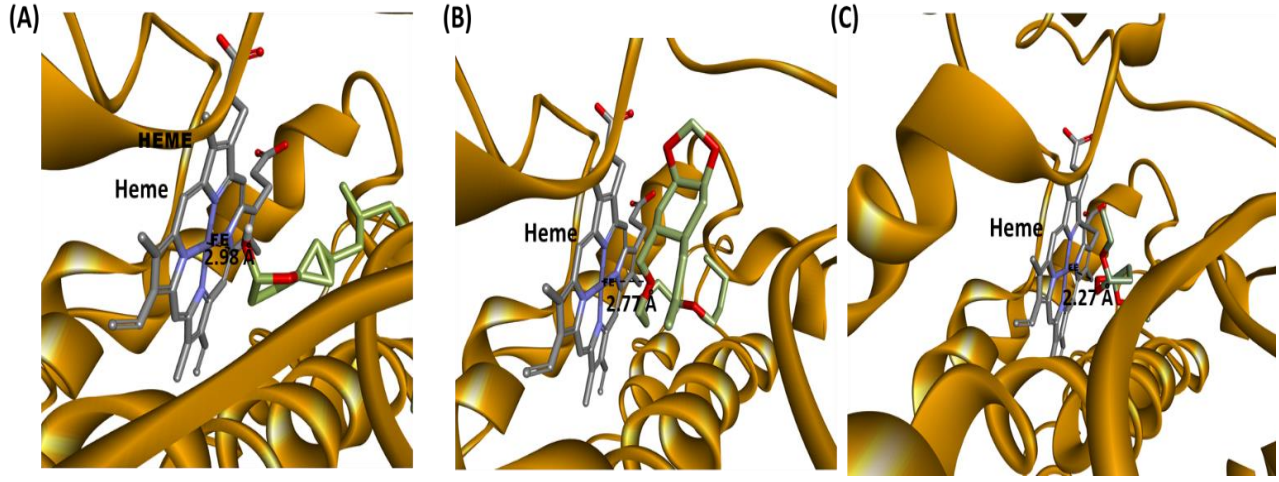

Figure 8. Analysis of binding mode of ligands following 50 ns MD simulation: (A) compound 5; (B) compound 8; and (C) compound 9.

Discussion

Computational studies using molecular docking and modelling are generally vital tools used by many researchers for new drug design and development. The docking simulations are also reported as a useful tool, illustrating for example, the cytochrome P450 isoforms that can metabolize insecticides. The docking simulation can also rationalize the observed heterogeneities of substrate preferences and metabolism detected among the P450 enzymes family [(62)(63)]. In the absence of crystal structure of P450 isoform, the knowledge of the molecular structure of the insect P450s have only been possible through homology modelling [(40)]. *In silico* homology modelling study is an explanatory tool rather than predictive tool [(64)], and can be used to investigate structure-function of the enzyme targets.

The docking scores showed promising inhibitory potentials of some pytoligand from *F. sycomorus* active fraction against *CYP6P3* isoform. Out of the 10 compounds assessed, only 4 ligands fitted into active site of the enzyme— 3 of which formed contacts with the central heme iron, whereas the rest were too big to fit in the active site of *CYP6P3*. Several studies have revealed that the molecular properties that impact the binding of a substrates are the ligand linear planarity, the Highest Occupied Molecular Orbital (HOMO) energy, Phe residue $\pi - \pi$ stacking, optimum placement of acceptor and donor substituent for interaction with the polar residues in the active site, and desolvation (ClogP) [(65)(66)]. The ligand/molecule planarity (area/depth2 ratio) and molecular mass were established to be the vital requisites for ligand to be particularly P450s substrates/inhibitors. The chemistry of the *F. sycomorus* ligands used in this study showed that they have a relative molecular mass ranging from 198-562 Da.

Compounds 5, 8, and 9 docked well into the active site of *CYP6P3*, whereas compounds 3, 4, 6 and 7 were practically unfit due to steric clashes. Due to the rigid protein target approximation used in Glide programs, the ligands with steric clashes for a specific protein conformation are not good scorers. These ligands are referred to as non-inhibitors of *CYP6P3*. This may be due certain factors, such as, the rotamer side chain that may obstruct ligand atoms from binding to their favored spot in the binding site. The fitting ligands are ranked by Glide XP whereas the unfitting ligands need an induced-fit *modus operandi* [(67)(68)] to suitably assess their binding affinities [(69)].

The best distance linking the substrate/inhibitor atom of oxidation to the heme iron atom (4.0 Å - 7.5 Å range) is regarded as the important yardstick for determining the best mode of inhibitor/substrate binding. The 6.0 Å distance or less between the heme iron and an atom in the substrate/inhibitor were marked as reactive since activation of the C-H bond by the heme-Fe-O reaction complex during catalysis is likely [(70)]. A general method to identify a successful docking pose of P450 is to necessitate that an inhibitor/substrate's site of metabolism (SOM) is within a specific range or distance from the heme central iron in a state of lowest binding energy conformation. Frequently, the maximum distance of 6 Å were suggested [(71)(72)]. A lengthy distance from the heme iron produces a wide area above the heme plane in P450 structures which subsequently allowed room for other inhibitors/substrate atoms besides the SOM. This paves way for error prone process of identifying the SOM due to present of multiple substrate atoms at the active sites.

The P450s have quite number of potentials inhibition stages in their reaction cycle, Viz: substrate binding, ferric (Fe^{3+}) to ferrous (Fe^{2+})(one electron) reduction, oxygen binding to ferrous iron, second electron transfer to the ferrous-oxy-substrate complex and subsequent activated oxygen intermediate and water release, activated oxygen insertion to substrate and release of the oxygenated product and Ferric (Fe^{3+}) form of the P450s [(73)]. The substrate binding, Oxygen binding and transfer of activated oxygen to the substrate stages were more prone to inhibition [(74)]. Several reversible inhibitors act by coordinating with the prosthetic heme iron atom as depicted in figure 3. This

coordination shifts the heme-iron from the high to the low spin form producing a difference spectrum product [75]. The change in the iron spin state occurs concurrently with a change in the redox potential of the P450. This eventually makes reduction by the P450 reductase more difficult [76]. Thus, the inhibition of *CYP6P3* by these ligands is a consequence not only for the occupation of the sixth coordination site of the iron but also the altering the reduction potential of the heme central iron.

These phytoligands may also form quasi-irreversible complexes with the heme central iron-atom. Some inhibitor compounds such as alkyl and aryl methylenedioxyl classes are generally catalyzed by P450 to form intermediate species that tightly coordinate to the prosthetic group forming stable metabolite intermediate complexes (MI complexes) [77]. Another proposed inhibition mechanism of these phytoligands is that they may be oxidized by P450s to an electrophilic reactive intermediate, which forms covalent bonding with the enzyme protein structure causing mechanism-based inhibition [78][79].

Hydrophobic side chain has been proposed to strongly interact with hydrophobic substrate/inhibitor and support water displacement from the active sites during binding [80] as proposed in this study. Consequently, hydrophilic group in the ligands can maintain the iron in low spin state and prevent dislodgment of water molecules from the enzyme active site and thus, inhibiting its activities. The placement of water molecules that are directly involved in binding and the rigidity of side chains can dramatically influence the posing of ligands. And where conformational changes upon binding occur, rigid active sites are limited in their ability to predict poses [81]. This agreed with these study findings as hydrophilic groups from compounds 5, 8 and 9 interact with heme iron and probably maintaining the heme iron in stable low spin state and inhibit oxygen binding.

The computed LE decreases with increasing number of heavy atoms as previously observed by Reynolds et al. [54] and Reynolds et al.[82]. This is contrary to our finding which showed increase in LE with increase of heavy atoms. The contributing factors to the decrease LE for the larger ligands might be due to less favorable binding entropies for larger and flexible compounds [83]. Analysis of large numbers of protein-ligand complexes over a wide range of affinities [84] demonstrates that suitable/optimal, ligand efficiencies are analytically higher for small ligands than large ones. This agreed with the data of this study where compound 5 and 8 showed efficiency greater than 0.3Kcal/mol/HA and thus, can potentially be optimized. Fit Quality (FQ) and SILE convert LE into a metric that is more consistent across wide ranges of molecular size. Similarly, this approach has also been applied to derive size independent enthalpy efficiencies, where free energy is replaced by enthalpy [84]. Analysis of enthalpy and entropy efficiencies showed that the size dependency of a ligand is generally associated with enthalpy [85]. In addition, MD simulation revealed the potentially stable binding mode of compound 5, 8, and 9, thereby further validating both the docking and ligand optimization results.

Conclusion

Compounds 5, 8 and 9 bound to the Heme iron of *CYP6P3* at proximity less than the maximum distance required for reactivity (6 Å). The binding energies indicate non-spontaneous interaction and energy consuming process with the enzyme active site. The most common amino acid residues in the binding pocket were *Phe123, Val310, Pro379 and Val380.* Some reversible and irreversible inhibitors act by coordinating with the prosthetic heme iron atom and formation of quasi-irreversible complexes with the iron of the heme prosthetic group, respectively. The LE matrics showed high potential of these compounds (particularly, compound 5 and 8) to form core fragment for optimization into a potent P450s inhibitors via molecular tactics such as carbon atom replacement and lipophilic group addition. MD simulation performed for these complexes to assess the stability of ligand binding mode. The results show that in addition to being stable in the enzyme binding pocket, these

compounds maintained Fe^{2+}(Heme):O (Ligand) distance over time. Thus, these compounds could serve as potential insecticide synergists and/or provide scaffold for further optimization into potent *CYP6P3* inhibitors.

Acknowledgement

The authors were grateful to ***Tetfund*** for financially supporting the project.

Conflicts of interest

None declared

REFERENCES

(1) World Health Organization (WHO, 2014). *Division of Malaria and Other Parasitic Diseases. From Malaria Control to Malaria Elimination: A Manual for Elimination Scenario Planning.* World Health Organization; 2014.

(2) World Health Organization(WHO, 2013). *Larval source management: a supplementary measure for malaria vector control: an operational manual. Geneva: World Health Organization;* 2013. p. 116. Available from: www.who.int/malaria/publications/atoz/9789241505604/en/%0A%0A

(3)Rose, R.I. Pesticides and Public Health: Integrated Methods of Mosquito Management. *Emerg Infect Dis J.*, 2001; 7:17.

(4) Katagi, T. Photodegradation of pesticides on plant and soil surfaces. *Rev Environ Contam Toxicol.*, 2004; 182: 1-189.

(5) Feyereisen, R. Insect P450 enzymes. *Ann. Rev. Entomol*, 1999; 44: 507-533.

(6) Scott J. G. Cytochromes P450 and insecticides resistance. *Insect Biochem Mol Biol.* 1999; 29: 757-777.

(7) Holt, R. A., Subramanian, G. M., Halpern, A., Sutton, G. G., Charlab, R., Nusskern, D. R., Wincker, P., Clark, A. G., Ribeiro, J. C. and Wides, R. The genome sequence of the malaria mosquito *Anopheles gambiae*. *Science*, 2002; 298: 129-149.

(8) Nene, V., Wortman, J. R., Lawson, D., Haas, B., Kodira, C., Tu, Z. J., Loftus, B., Xi, Z., Megy, K. & Grabherr, M. Genome sequence of *Aedes aegypti*, a major arbovirus vector. *Science*, 2007; 316: 1718-1723.

(9) Arensburger, P., Megy, K., Waterhouse, R. M., Abrudan, J., Amedeo, P., Antelo, B., Bartholomay, L., Bidwell, S., Caler, E. & Camara, F. Sequencing of *Culex quinquefasciatus* establishes a platform for mosquito comparative genomics. *Science*, 2010; 330: 86-88.

(10) Nikou, D., Ranson, H. & Hemingway, J. An adult-specific CYP6 P450 gene is overexpressed in a pyrethroid-resistant strain of the malaria vector, *Anopheles gambiae*. *Gene*, 2003; 318: 91-102.

(11) David, J.P., Strode, C, Vontas, J., Nikou, D., Vaughan, A., Pignatelli, P.M., Louis, C., Hemingway, J., Ranson, H. The *Anopheles gambiae* detoxification chip: a highly specific microarray to study metabolic-based insecticide resistance in malaria vectors. *Proc Natl Acad. Sci.* 2005; 102 (11): 4080-4084. 10.1073/pnas.0409348102.

(12) Muller P, Donnelly MJ, Ranson H. Transcription profiling of a recently colonised pyrethroid resistant *Anopheles gambiae* strain from Ghana. *BMC Genomics*, 2007; 8: e36

(13) Mulamba, C., Irving, H., Riveron, J.M., Mukwaya, L.G., Birungi, J, Wondji, C.S. Contrasting *Plasmodium* infection rates and insecticide susceptibility profiles between the sympatric sibling species *Anopheles parensis* and *Anopheles funestus* s.s: a potential challenge for malaria vector control in Uganda. *Parasit Vect*., 2014; 7: 71.

(14) Mansuy, D. The great diversity of reactions catalyzed by cytochrome P450. *Comp Biochem Physiol Part C*, 1998; 121:5-14.

(15) Guengerich, F. P. Mechanisms of Cytochrome P450-Catalyzed Oxidations. *ACS Catal*., 2018; 8(12):10964–10976. doi:10.1021/acscatal.8b03401

(16) Correia, M. A., and Ortiz de Montello, P.R. *Inhibition of cytochrome P450 enzymes,* In P. R. Ortiz de Montello (ed.), *Cytochrome P450: Structure, Mechanism, and Biochemistry*, 3rd ed. Kluwer Academic/Plenym Publishers, New York. 2005; Pp 247-332.

(17) N'Guessan, R., A. Asidi, P. Boko, A. Odjo, M. Akogbeto, O. Pigeon, and Rowland, M. (2010). An experimental evaluation of PermaNet 3.0, a deltamethrin-piperonyl butoxide combination net, against pyrethroid-resistant *Anopheles gambiae* and *Culex quinquefasciatus* mosquitoes in southern Benin. *Trans. R. Soc. Trop. Med. Hyg*. 2010; 104: 758-765.

(18)Tungu, P., S. Magesa, C. Maxwell, R. Malima, D. Masue, W. Sudi, J. Myamba, O. Pigeon, and Rowland, M. Evaluation of PermaNet 3.0 a deltamethrin-PBO combination net against *Anopheles gambiae* and pyrethroid resistant *Culex quinquefasciatus* mosquitoes: an experimental hut trial in Tanzania. *Malar. J.*, 2010; 9: 21.

(19) Darriet, F. and Chandre. F. Combining piperonyl butoxide and dinotefuran restores the efficacy of deltamethrin mosquito nets against resistant *Anopheles gambiae* (Diptera: Culicidae). *J. Med. Entomol*. 2011; 48: 952-955.

(20) Anosike, C.A., Babandi, A. and Ezeanyika, L.U.S. Potentiation Effects of *Ficus sycomorus* Active Fraction Against Permethrin-Resistant Field-Population of *Anopheles coluzzii* (Diptera: Culicidae). *Neotrop. Entomol*., 2021; 50: 484-496.

(21) Tanaka, T, Fujitani, T, Takahashi, O, Oishi, S. Developmental toxicity evaluation of piperonyl butoxide in CD-1 mice. *Toxicol Lett*. 1994; 71:123–129.

(22) Takahashi, O, Oishi, S, Fujitani, T, Tanaka, T, Yoneyama, M. Chronic toxicity studies of piperonyl butoxide in CD-1 mice: Induction of hepatocellular carcinoma 1. *Toxicology*, 1997; 124: 95–103.

(23) Djouaka, R. F., Bakare, A. A., Coulibaly, O. N., Akogbe T.O.M.C., Ranson, H., Hemingway, J. and Strode, C. Expression of the cytochrome P450s, CYP6P3 and CYP6M2 are significantly elevated in multiple pyrethroid resistant populations of *Anopheles gambiae* s.s. from Southern Benin and Nigeria. *BMC Genomics*, 2008; 9: 538.

(24) Muller, P, Warr, E, Stevenson, B.J, Pignatelli, P.M, Morgan, J.C, Steven, A. et al. Field-caught permethrin-resistant *Anopheles gambiae* over-express CYP6P3, a P450 that metabolises pyrethroids. *PLoS Genet*. 2008; 4: e1000286.

(25) Edi, C.V., Djogbenou, L., Jenkins, M.A., Regna, K., et al. CYP6 P450 enzymes and ACE-1 duplication produce extreme and multiple insecticide resistance in the malaria mosquito *Anopheles gambiae*. *PLoS Genet*. 2014; 10: 1-12.

(26) Ranson, H. and Lissenden, N. Insecticide resistance in African Anopheles mosquitoes: a worsening situation that needs urgent action to maintain malaria control. *Trends in Parasitol.*, 2016; 32:187–96.

(27) Miresmailli, S. and Isman, M.B. Botanical insecticides inspired by plant-herbivore chemical interactions. *Trends in Plant Sci*., 2014; 19:29-35.

28) Biondi, A., Mommaerts, V., Smagghe, G., Viñuela, E., Zappalà, L., Desneux, N. The non-target impact of spinosyns on beneficial arthropods. *Pest Mgt. Sci.*, 2012; 68:1523-1536.

(29) Rhome, A.A. Phytochemicals from *Ficus sycomorus* L. leaves act as insecticides and acaricides. *African J Agric Res*; 2013; 8(27):3571–9. *doi*: 10.5897/AJAR2013.7243.

(30) Govindarajan, M. Larvicidal and repellent properties of some essential oils against *Culex tritaeniorhynchus* Giles and *Anopheles subpictus* Grassi (Diptera: Culicidae). *Asian Pac J. Trop Med*., 2010; 4:106–111.

(31) Pavela, R. Acute toxicity and synergistic and antagonistic effects of the aromatic compounds of some essential oils against *Culex quinquefasciatus* Say larvae. *Parasitol. Res*., 2015; 114: 3835–3853.

(32) Pavela, R and Benelli, G. Essential oils as eco-friendly biopesticide? Challenges and constraints. *Trend Plant Sci*., 2016; 21:1000-1007.

(33) Sedjati, S., Ambariyanto, A., Trianto A., Supriyantini, E., Ridlo, A., Yudiati, E., Firmansyah, T. Anti-Vibrio from Ethyl Acetate Extract of Sponge-Associated Fungus *Trichoderma longibrachiatum*. ***Jordan Journal of Pharmaceutical Sciences***, 2021; 4:435-443

(34) Ali, H., Alkowni, N., Jaradat, N., Masri, M. Evaluation of phytochemical and pharmacological activities of *Taraxacum syriacum* and *Alchemilla arvensis*. ***Jordan Journal of Pharmaceutical Sciences***, 2021; 14(4):457-471.

(35) Perumalsamy, H., Chang, K.S., Park, C. and Ahn, Y. J. Larvicidal activity of compounds isolated from *Asarum heterotropoides* root constituents against insecticide-susceptible and -resistant *Culex pipiens pallens*, and *Aedes aegypti* and *Ochlerotatus togoi. J. Agric. Food Chem*. 2010; 58:10001-10006.

(36) Wang, Z., Kim, J. R., Wang, M., Shu, S. and Ahn, Y. J. Larvicidal activity of *Cnidium monnieri* fruit coumarins and structurally related compounds against insecticide susceptible and -resistant *Culex pipiens pallens* and *Aedes aegypti. Pest Mgt Sci*., 2012; 68:1041-1047.

(37) Pethuan, S., Duangkaew, P., Sarapusit, S., Srisook, E. and Rongnopart, P. Inhibition against Mosquito cytochrome P450 enzymes by Rhinacanthin-A, -B, and -C elicits synergism on cypermethrin cytotoxicity in *Spodoptera frugiperda* Cells. *J. Med. Entomol*., 2012; 49(5): 992-1000.

(38) Abdel-Tawab H.M., Samia, M.M.M. and Natarajan, C. Safety of Natural Insecticides: Toxic Effects on Experimental Animals. *Biomed Res. Int*. 2018:1-17. https://doi.org/10.1155/2018/4308054.

(39) Antonious, G.F. Residues and half lives of pyrethrins on field- grown pepper and tomato. *J. Environ. Sci. Health B.*, 2004; 39:491–503.

(40) Jones, R. T., Bakker, S. E., Stone, D., Shuttleworth, S. N., Boundy, S., Mccart, C., Daborn, P. J. and Van Den Elsen, J. M. Homology modeling of *Drosophila* cytochrome P450 enzymes associated with insecticide resistance. *Pest Mgt. Sci.*, 2010; 66**:**1106-1115.

(41) de Graaf, C. Cytochrome P450-Drug interactions computational binding mode and affinity predictions in CYP2D6. PhD thesis, Department of Chemistry and Pharmacochemistry, Vrije Universiteit Amsterdam, De Boelelaan 1083, 1081 HV Amsterdam, The Netherlands.2006.

(42) Magrane, M. and Consortium, U. *UniProt Knowledgebase: a hub of integrated protein data.* Database (Oxford), 2011: P. 9.

(43) Kuhnel, K., Ke, N., Cryle, M.J., Sligar, S.G., Schuler, M.A., Schlichting, I. Crystal Structures of Substrate-Free and Retinoic Acid-Bound Cyanobacterial Cytochrome P450 Cyp120A1. *Biochemistry*, 2008; 47: 6552.

(44) Webb, B. and Sali, A. *Comparative Protein Structure Modeling Using Modeller. Current Protocols in Bioinformatics* 54, John Wiley & Sons, Inc., 5.6.1-5.6.37, 2016, P 54.

(45) Friesner, R. A.; Banks, J. L., Murphy, R. B., Halgren, T. A., Klicic, J. J., Mainz, D. T., Repasky, M. P., Knoll, E. H., Shelley, M.., Perry, J. K., Shaw, D. E., Francis, P., Shenkin, P. S. Glide: A new approach for rapid, accurate docking and scoring. 1. Method and assessment of docking accuracy. *J. Med. Chem*., 2004; 47:1739-1749.

(46) Caporuscio, F., Rastelli, G.; Imbriano, C., del Rio, A. Structure-based design of potent aromatase inhibitors by high-throughput docking. *J. Med. Chem*. 2011; 54: 4006–4017.

(47) Abdul-Hay, S.O., Lane, A.L., Caulfield, T.R., Claussin, C., Bertrand, J., Masson, A., Choudhry, S., Fauq, A.H., Maharvi, G.M., Leissring, M.A. Optimization of peptide hydroxamate inhibitors of insulin-degrading enzyme reveals marked substrate-selectivity. *J. Med. Chem*., 2013; 56:2246–2255.

(48) Harder, E., Damm, W., Maple, J., Wu, C., Mark, R., Jin, Y. X., Wang, L., et al. (2016). OPLS3: A Force Field Providing Broad Coverage of Drug-like Small Molecules and Proteins. *J. Chem. Theory Comput.*, 2016; 12(1):281-296.

(49) Onawole, A. T., Sulaiman, K. O., Adegoke, R. O., and Kolapo, T. U. Identification of potential inhibitors against the Zika virus using consensus scoring. *J. Mol. Graphics Model*., 2017; 73:54–61. https://doi.org/10.1016/j.jmgm.2017.01.018.

(50) Kuntz, I. D., Chen, K., Sharp, K. A., Kollman, P. A. The maximal affinity of ligands. *Proc. Nat. Acad. Sci.*, U. S. A. 1999; 96: 9997-10002.

(51) Shultz, M.D. Setting expectations in molecular optimizations: strengths and limitations of commonly used composite parameters. *Bioorg. Med. Chem. Lett*. 2013; 23: 5980−5991.

(52) Hopkins, A. L., Groom, C.R., Alex, A. Ligand efficiency: a useful metric for lead selection. *Drug Discov. Today*, 2004; 9:430-1.

(53) Leeson, P.D. and Springthorpe B. The influence of drug-like concepts on decision-making in medicinal chemistry. *Nat. Rev. Drug Discov.* 2007; 6: 881–890.

(54) Reynolds, C. H., Bembenek, S. D., Tounge, B. A. The role of molecular size in ligand efficiency. *Bioorg. Med. Chem. Lett.* 2007; 17: 4258-4261.

(55) Nissink, J. W. M. Simple size-independent measure of ligand efficiency. *J. Chem. Inf. Model.* 2009; 49:1617-22.

(56) Lee, J., Cheng, X., Swails, J,M., Yeom, M.S., Eastman, P.K., Lemkul, J.A., et al. CHARMM-GUI Input Generator for NAMD, GROMACS, AMBER, OpenMM, and CHARMM/OpenMM Simulations Using the CHARMM36 Additive Force Field. *J. Chem. Theory and Comput.*, 2016; 12(1):405-413.

(57) Kim, S., Lee, J., Jo, S., Brooks, C.L., Lee, H.S. and Im, W. CHARMM-GUI ligand reader and modeler for CHARMM force field generation of small molecules. *J. Comput. Chem*., 2017; 38(21):1879-1886.

(58)Phillips, J. C., Braun, R., Wang, W., Gumbart, J., Tajkorshid, E., Villa, E., et al. Scalable molecular dynamics with NAMD. *J. Comput. Chem*. 2005; 26(16):1781-1802.

(59) Pettersen, E. F., Thomas, D.G., Conrad, C.H., Gregory, S.C., Daniel, M.G., Elaine, C.M., et al. UCSF Chimera-A visualization system for exploratory research and analysis. *J. Comput. Chem*. 2004; 25(13):1605-1612.

(60) Uba, A. I., Weako J., Keskin, Ö., Gürsoy, A., Yelekçi, K. Examining the stability of binding modes of the co-crystallized inhibitors of human HDAC8 by molecular dynamics simulation. *J. Biomol. Struct. Dyn*. 2020; 38(6):1751-1760. doi: 10.1080/07391102.2019.1615989.

(61) Uba, A. I., Yelekçi, K. Crystallographic structure versus homology model: a case study of molecular dynamics simulation of human and zebrafish histone deacetylase 10. *J. Biomol. Struct. Dyn*. 2020; 38(15): 4397-4406. doi: 10.1080/07391102.2019.1691658.

(62) Chandor-Proust, A., Bibby, J., Regent-Kloeckner, M., Roux, J., Guittard-Crilat, E., Poupardin, R., Riaz, M.A., Paine, M., Dauphin-Villemant, C., Reynaud, S., David, J.P. The central role of mosquito cytochrome P450 CYP6Zs in insecticide detoxification revealed by functional expression and structural modelling. *Biochem. J*. 2013; 455:75e85.

(63) McLaughlin, L.A., Niazi, U., Bibby, J., David, J.P., Vontas, J., Hemingway, J., Ranson, H., Sutcliffe, M.J., Paine, M.J. Characterization of inhibitors and substrates of *Anopheles gambiae CYP6Z2*. *Insect Mol. Biol*. 2008; 17:125e135.

(64) Szklarz, G. D., He, Y. A. and Halpert, J. R. Site-directed mutagenesis as a tool for molecular modeling of cytochrome P450 2B1. *Biochemistry*, 1995; 34**:**14312-14322.

(65) Lewis, D.F., Lake, B.G. and Dickins, M. Quantitative structure-activity relationships (QSARs) in inhibitors of various cytochromes P450: The importance of compound lipophilicity. *J. Enzym. Inhib. Med. Chem*., 2007; 22:1–6.

(66) Sridhar, J., Ellis, J., Dupart, P., Liu, J., Stevens, C.L., Foroozesh, M. Development of flavone propargyl ethers as potent and selective inhibitors of cytochrome P450 enzymes 1A1 and 1A2. *Drug Metab. Lett*., 2012; 6:275–284.

(67) Farid, R., Day, T., Friesner, R. A., Pearlstein, R. A. New Insights about HERG Blockade Obtained from Protein Modeling, Potential Energy Mapping, and Docking Studies. *Bioorg. Med. Chem.*, 2006; 14:3160-3173.

(68) Sherman, W., Day, T., Jacobson, M. P.; Friesner, R. A. and Farid, R. Novel Procedure for Modeling Ligand/Receptor Induced Fit Effects. *J. Med. Chem.*, 2006; 49:534-553.

(69) Krovat, E. M., Steindl, T., Langer, T. Recent Advances in Docking and Scoring. *Curr. Comput.-Aided Drug Des*. 2005; 1: 93-102.

(70) Meunier, B., de Visser, S. P., Shaik, S. Mechanism of oxidation reactions catalyzed by cytochrome P450 enzymes. *Chem Rev*, 2004; 104:3947-3980.

(71) Hritz, J., deRuiter, A., and Oostenbrink, C. Impact of plasticity and flexibility on docking results for cytochrome P4502D6: a combined approach of molecular dynamics and ligand docking. *J. Med. Chem*. 2008; 51:7469–

7477.doi: 10.1021/jm801005m.

(72) Vasanthanathan, P., Hritz, J., Taboureau, O., Olsen, L., Jørgensen, F.S., Vermeulen, N.P., et al. Virtual screening and prediction of site of metabolism for cytochrome P4501A2 ligands. *J. Chem. Inf. Model.* 2009; 49:43–52. doi: 10.1021/ci800371f.

(73) White, R.E.; Coon, M.J. Oxygen Activation by Cytochrome P450. *Ann. Rev. Biochem*., 1980; 49:315–356.

(74) Ortiz de Montellano, P.R.; Correia, M.A. *Inhibition of Cytochrome P450 Enzymes. In Cytochrome P450: Structure, Mechanism, and Biochemistry*; 2nd Ed.; Ortiz de Montellano, P.R., Ed.; Plenum Press: New York, 1995; Pp305–364.

(75) Schenkman, J.B., Sligar, S.G., Cinti, D.L. Substrate Interactions with Cytochrome P-450. *Pharmacol. Ther*., 1981; 12:43–71.

(76) Guengerich, F.P. Oxidation–Reduction Properties of Rat Liver Cytochromes P450 and NADPH-Cytochrome P-450 Reductase Related to Catalysis in Reconstituted Systems. *Biochemistry*, 1983; 22: 2811–2820.

(77) Hollenberg, P.E. Characteristics and common properties of inhibitors, inducers, and activators of cyp enzymes. *Drug Metab Rev*, 2002; 34(1&2):17–35.

(78) Pelkonen, O., Turpeinen, M., Hakkola, J., Honkakoski, P., Hukkanen, J., and Raunio, H. Inhibition and induction of human cytochrome P450 enzymes: current status. *Arch. Toxicol.*, 2008; 82:667–715.doi:10.1007/s00204-008- 0332-8.

(79) Orr, S.T., Ripp, S.L., Ballard, T.E., Henderson, J.L., Scott, D.O., Obach, R.S., et al. Mechanism-based inactivation (MBI) of cytochrome P450 enzymes: structure-activity relationships and discovery strategies to mitigate drug-drug interaction risks. *J. Med. Chem.* 2012; 55:4896–4933.doi:10.1021/jm300065h.

(80) Nickerson, D.P., Hardford-Cross, C.F., Fulcher, S.R., Wong, L.L. The catalytic activity of cytochrome P450 (cam) toward styrene oxidation is increased by site specific mutagenesis. *FEBS Lett*., 1997; 405:153-156.

(81) Kitchen, D.B., Decornez, H., Furr, J.R., Bajorath, J. Docking and scoring in virtual screening for drug discovery: Methods and applications. *Nature Rev Drug Discov.*, 2004; 3: 935–949.

(82) Reynolds, C. H., Tounge, B.A., Bembenek, S.D. Ligand binding efficiency: trends, physical basis, and implications. *J. Med. Chem.* 2008; 51: 2432-8.

(83) Loving, K., Alberts, I., Sherman, W. Computational approaches for fragment-based and de novo design. *Curr. Top. Med. Chem.* 2012; 10: 14-32.

(84) Ferenczy, G. G., Keseru, G. M. Enthalpic efficiency of ligand binding. *J. Chem. Inf. Mod.* 2010; 50:1536-1541.

(85) Reynolds, C. H., Holloway, M. K. Thermodynamics of Ligand Binding and Efficiency. *ACS Med. Chem. Lett*. 2011; 2: 433-7.

دراسات النمذجة الجزيئية لبعض النباتات النباتية من جزء Ficus sycomorus كمثبطات محتملة لإنزيم السيتوكروم CYP6P3 من Anopheles coluzzi

أبا بابانديي[1،2*] ، شيوما أ. أنوسيك[2]، لورنس إزانييكا[2]، كمال يلكجي[3]، عبد الله إبراهيم أوبا[4*]

[1] قسم الكيمياء الحيوية جامعة بايرو، نيجيريا.

[2] قسم الكيمياء الحيوية، جامعة نيجيريا، نيجيريا.

[3] قسم المعلوماتية الحيوية وعلم الوراثة ، كلية الهندسة والعلوم الطبيعية ، جامعة قادر هاس، تركيا.

[4] قسم النظم المعقدة، مركز بكين لبحوث العلوم الحاسوبية، الصين.

ملخص

العقبة الرئيسية في مكافحة الملاريا هي مقاومة البعوض للمبيدات الحشرية، بما في ذلك البيرثرويد. ترجع المقاومة بشكل أساسي إلى الإفراط في التعبير عن إنزيمات إزالة السموم مثل السيتوكرومات. يمكن تقليل تحمل المبيدات الحشرية عن طريق مثبطات P450s المشاركة في إزالة السموم من المبيدات الحشرية. هنا، لتصميم مثبطات CYP6P3 المحتملة، تم إنشاء نموذج تماثل للإنزيم باستخدام التركيب البلوري للبكتيريا الزرقاء المرتبط بحمض الريتينويك CYP120A1 (معرف PDB: 2VE3 ؛ القرار: 2.1 Å). تم استخدام دراسة الالتحام الجزيئي والنمذجة الحسابية لتحديد الإمكانات المثبطة لبعض النباتات النباتية المعزولة من Ficus sycomorus ضد Anopheles coluzzii النموذجي P450، CYP6P3 ، المتورط في المقاومة. تم تحليل خصائص تحسين الترابط المحتمل (LE) باستخدام النماذج الرياضية القياسية. المركبات 5 و 8 و 9 مرتبطة بحديد Heme لـ CYP6P3 ضمن 3.14 و 2.47 و 2.59 Å، على التوالي. قدرت طاقات الارتباط الخاصة بكل منها بـ −8.93 و −10.44 و −12.56 كيلو كالوري / مول. لفحص ثبات وضع الربط الخاص بهم، تم إخضاع مجمعات الالتحام الناتجة من هذه المركبات باستخدام CYP6P3 لمحاكاة 50 نانوثانية MD. ظلت المركبات مرتبطة بالإنزيم و Fe (Heme): يبدو أن مسافة O (Ligand) قد تم الحفاظ عليها بمرور الوقت. يؤدي التنسيق بين ليجند قوي إلى حديد الهيم إلى تحويل الحديد من الشكل العالي إلى شكل الدوران المنخفض المستقر ومنع الأكسجين من الارتباط بالهيم وبالتالي تثبيط النشاط التحفيزي. أظهر مؤشر LE القدرة العالية لهذه المركبات (5 و 8) لتوفير جزء أساسي لتحسين مثبطات P450 القوية.

الكلمات الدالة: نمذجة التنادد. CYP6P3؛ الالتحام الجزيئي كفاءة يجند محاكاة الديناميات الجزيئية؛ مثبطات CYP6P3.

---

* ***المؤلف المراسل: أبا بابانديي، عبد الله إبراهيم أوبا***

ababandi.bch@buk.edu.ng , aiuba@csrc.ac.cn

تاريخ استلام البحث 2021/8/25 وتاريخ قبوله للنشر 2021/12/26.